Catal Lett (2009) 131:632–642
DOI 10.1007/s10562-009-0008-x

Sodium Hydroxide–Sodium Oxalate-Assisted Co-Precipitation of Highly Active and Stable Cu/ZrO_2 Catalyst in the Partial Oxidation of Methanol to Hydrogen

Hongwei Chen · Anyuan Yin · Xiuying Guo ·
Wei-Lin Dai · Kang-Nian Fan

Received: 30 March 2009 / Accepted: 29 April 2009 / Published online: 23 May 2009

Abstract The Cu/ZrO_2 catalysts prepared by the co-precipitation with $NaOH–Na_2C_2O_4$ mixture solution exhibited high activity and stability in the hydrogen production through partial oxidation of methanol. The methanol conversion and the selectivity to hydrogen can be up to 100 and 92% at 533 K with molar ratio of O_2/CH_3OH at 0.5, respectively. Characterization results indicated that CuO were well dispersed into the ZrO_2 lattices which induced the strong Cu–Zr interaction as well as good stability and lower valance of Cu species were supposed as the activate sites. The good catalytic performance and long-term stability of the novel Cu/ZrO_2 catalysts could be attributed to the high copper species dispersion on zirconium components and high active specific copper surface area with a much strong Cu–Zr interaction as well as a beneficial synergy of ZrO_2 promotion.

Keywords Partial oxidation of methanol ·
Hydrogen production · Cu/ZrO_2 catalyst ·
Catalyst characterization

1 Introduction

Proton-exchange membrane fuel cells (PEMFC), for their good advantages of non-pollution and accordance with the green-chemistry on energy application, appear to be the most promising technology for power application, and especially can be used to supply energy for the vehicle [1]. Among all the candidates, H_2 is considered to be the most clean energy source for PEMFC. However, the mass-produced hydrogen remains to be investigated considering the convenience of handling and the economic evaluations. It is commonly accepted that methanol can be used as a good H_2 reservoir since methanol can be easily accessed, and it has the second highest available hydrogen in the organic compounds only lower than methane. In addition, methanol has no C–C bonds, thus the coke formation on the surface of catalysts can be minimized [2, 3].

Hydrogen can be obtained from methanol by different routes. The simplest method is the endothermic decomposition of methanol (MD) that induced a gas production of 1:2 (mol/mol) CO and H_2 mixtures [4, 5]. Because CO can lead to the poisoning of the Pt anodes of PEMFC, the gas mixture must be retreated to remove the small amounts of CO until its content is lower than the level which can not poison the Pt anodes (<50 ppm). Methanol steam reforming (MSR) [1, 6] is much efficient to produce hydrogen accompanied with little CO content which may be applied to PEMFC. The disadvantage of this method remains the same character of endothermic decomposition of MD which needs additional energy from the environment to maintain the reaction.

There is still another route to obtain hydrogen from methanol through partial oxidation of methanol (POM) [7–13] or oxidative steam reforming of methanol (OSRM) [14, 15]. OSRM processes usually need long warm-up time and external heat sources, which creates problems for portable applications. POM reaction is an exothermic reaction, which can be easily self-sustained. But the drawback of POM compared to MSR is that the CO content in the tail gas is higher than that in MSR which limited its application in PEMFC.

H. Chen · A. Yin · X. Guo · W.-L. Dai (✉) · K.-N. Fan
Department of Chemistry & Shanghai Key Laboratory of Molecular Catalysis and Innovative Materials, Fudan University, Shanghai 200433, People's Republic of China
e-mail: wldai@fudan.edu.cn

Over the last two decades, increasing attention has been paid to the POM to produce high-purity hydrogen used in fuel cells for on-board power generation for vehicles. This application requires catalysts with high activity, selectivity, and stability under reaction conditions. Numerous Cu/ZnO-based catalysts with various modifications have been tested [7, 8, 10, 12]. Eswaramoorthi et al. [16] reported that the catalysts applied in MSR could also applied in POM, and some Cu-based catalysts including Cu/ZnO and Cu/ZnO/Al_2O_3 were tried, but the stability and the CO selectivity were still not suitable for PEMFC application [1, 6]. Recently, ZrO_2 as an attractive support material or promoter for the activation and stabilization of copper other than ZnO or alumina is well documented in the field of methanol synthesis [17–20], mainly due to its unique amorphous character and redox properties. de Lima et al. [20] studied the effects of active phases and supports on the catalytic performance of partial oxidation of methanol, with Cu/ZnO producing more CO_2 and Pt/ZrO_2 producing more CO. Eduardo [21] studied the effect of the promoters such as Ce, Pd, Zr on the catalytic performance of Cu/ZnO-based catalyst in the partial oxidation of methanol, and reported the introduction of zirconium can improve the catalytic performance obviously, of which the Cu/ZrO_2/ZnO catalyst exhibited higher stability in the 100 h life time experiment. Pokrovski and Bell [22] studied the effect of dopants on the activity of Cu/ZrO_2 for CO hydrogenation to methanol and concluded that the zirconium dioxide support supplied adequate bridge-bonded hydroxyl groups which contributed to the rapid release of methoxide groups formed on the oxide surface and formation of methanol. Robert et al. [23] reported the Cu/ZrO_2 catalyst prepared by sol–gel method exhibited good catalytic performance in the SRM. Yao et al. [3] reported that Cu/ZrO_2 show much better activity than Cu/ZnO and Cu/ZnO/Al_2O_3 for the MSR reaction due to strong Cu–Zr interaction, good reducibility and better dispersion of Cu or CuO. Moreover, ZrO_2 was known to possess anionic vacancies, which entails a geometric effect that can influence the dispersion and lead to a change in the morphology of the supported copper particle [22]. The Cu/Zr mole ratio can also influence the activity very much [24].

To date, numerous technical methods such as incipient wet impregnation [3], oxalate gel-coprecipitation [3], microemulsion technique [25], traditional aqueous coprecipitation [3], and sol–gel processes have been developed to prepare Cu/ZrO_2 mixed oxide catalysts for various applications. Among these techniques, oxalate gel-coprecipitation and sol–gel processes have shown to be efficient for preparing the copper-based catalysts. However, these processes often have disadvantages, such as tedious multistep processing and the need for delicate pH control. In addition, the cost of the Cu/ZrO_2 catalyst is high and limits its further application into the industry. To circumvent these problems, the development of new practical and effective methods for preparation of the Cu/ZrO_2 catalyst with high copper dispersion and strong copper–zirconium interaction is highly desired.

In this study, for the first time, we report a novel Cu/ZrO_2 system derived from NaOH–$Na_2C_2O_4$ assisted co-precipitation method, which showed good activity and stability in the hydrogen production of POM. Because the effects of the NaOH–$Na_2C_2O_4$ on the catalytic performance in the POM process have discussed in previous study [26], special attention is paid to the effects of the mol ratio of Cu/Zr on their structural properties and catalytic behavior in the POM process. The intrinsic relationship between the structure and the catalytic performance were discussed on the basis of XRD, BET, TPR, SEM, TEM and XPS analyses.

2 Experimental

2.1 Preparation of Catalyst

Cu/ZrO_2 catalysts with different Cu/Zr mole ratios were prepared by Sodium hydroxide–sodium oxalate-assisted co-precipitation method. A typical procedure for preparing the catalyst precursor is as follows. First, the solution of $Na_2C_2O_4$–NaOH with mole ratio of 1/2 ($Na_2C_2O_4$, 0.5 M) was pumped slowly into the mixed copper nitrite and zirconium nitrate at room temperature under vigorous stirring. During the precipitation, the temperature was maintained at 333 K. Then, the precipitates were filtered and washed until the pH value of the filtrates were around 7.0 and dried at 373 K overnight. Finally, calcination of the as-obtained materials was performed in a muffle oven at 723 K for 4 h. The as-prepared catalysts are named as CZx according to the mole ratio of Cu/Zr. For instance, catalyst CZ1, CZ2, CZ3, CZ4 represented mole ratio of Cu/Zr at 1/4, 2/3, 3/2 and 4/1, respectively.

2.2 Catalyst Characterization

The BET specific surface areas of the calcined samples were determined by adsorption–desorption of nitrogen at liquid nitrogen temperature, using Micromeritics TriStar 3000 equipment. Sample degassing was carried out at 573 K prior to acquiring the adsorption isotherm. The powder X-ray diffraction (XRD) measurement was carried out on a Bruker D8 Advance X-ray diffractometer using nickel filtered Cu Kα radiation (1.5406 Å) with a scanning angle (2θ) of 15–80°, a scanning speed of 0.84° min^{-1}, a voltage and current of 40 kV and 20 mA, respectively. Before being transferred into the chamber, the samples dispersed in ethanol were deposited on the sample holder and then quickly moved into the vacuum chamber. TPR measurements were carried out on a homemade apparatus as described elsewhere. About 20 mg of a freshly calcined catalyst was mounted in a quartz tube. TPR experiments were carried out in 5% H_2/Ar flowing at 40 mL min^{-1}, with a ramping rate of 10 K min^{-1}. The special surface area of metallic copper was measured by the pulse titration technique of N_2O on the surface of metallic copper as follows: $2Cu(s) + N_2O \rightarrow N_2 + Cu_2O(s)$. Pure nitrogen was used as the carrier gas, and a thermal conductivity detector (TCD) was used to detect the consumption of N_2O. The specific active surface area of metallic copper was calculated from the total amount of N_2O consumption with 1.46×10^{19} copper atoms per m^2. XPS test was performed by a Perkin–Elmer PHI 5000C ESCA system equipped with a hemispherical electron energy analyzer. The Al Kα ($h\nu = 1486.6$ eV) was operated at 14 kV and 20 mA. The carbonaceous C 1s line (284.6 eV) was used as the reference to calibrate the binding energies (BEs). To investigate the nature of Cu species on the surface of the reduced catalysts as well as the ones after POM reaction, XPS characterizations after reduction and reaction were also performed. The POM reaction was carried out ex situ in a vertical down-flow reactor, similar to that used for the catalytic experiments, after that the samples were cooled to room temperature. Then the samples were pressed to a self-supported disk and was degassed in the pretreatment chamber in vacuum before being transferred into the analyzing chamber where the background pressure was better than 2×10^{-7} Pa.

2.3 Activity Tests

The catalytic activity evaluation was performed at atmospheric pressure in a fixed-bed flow micro-reactor. The catalyst was diluted with quartz sands to avoid adverse thermal effects. All the calcined precursors were crushed into 60–80 meshes, and 0.3 g of the catalyst diluted with quartz sand (60–80 meshes) was packed in a stainless steel tubular reactor. The sample was reduced by H_2/Ar (5% H_2) at 523 K for 2 h under the flowing rate of 300 mL min^{-1}. After that, methanol was pumped into the pre-heater and then mixed with O_2 controlled in the appointed O_2/MeOH ratio by a mass flow controller. The vaporized feed then entered the reactor tube with a stream of argon gas at a flow velocity of 30 mL min^{-1} to initiate the POM reaction at the desired reaction temperature. The reaction products were firstly passed through a cold trap, then the gaseous products, such as H_2, CO, CO_2 and CH_4 were detected online by a gas chromatograph (GC-122, Shanghai Analysis) equipped with a TCD detector and a TDX-01 column; the liquid products such as water, methanol were detected by the same GC equipped with a TCD and a Porapak-Q column. Unless otherwise specified, the catalytic activity was evaluated from the data collected between 5 and 6 h of the on-stream operation by methanol conversion (C_{MeOH}), CO_2 selectivity (S_{CO_2}) and H_2 selectivity ($*\Sigma_H$) in the outlet. Catalyst turnover frequencies (TOFs, in s^{-1}) were calculated as the number of hydrogen molecules produced per surface copper atom, as determined by the nitrogen oxide decomposition measurements described above.

3 Results and Discussion

3.1 XRD

The XRD patterns of CZ*x* catalysts and the catalysts after the POM reactions are shown in Fig. 1. Figure 1a shows the XRD patterns of the calcined catalyst precursors with different mole ratio of Cu/Zr. For pure ZrO_2, the principal peak seen at 30.3° in the diffraction pattern can be ascribed to tetragonal ZrO_2 (t-ZrO_2), with a trace of monnclinic ZrO_2 (m-ZrO_2) evident at 28.5° and 31.2°. The volume fraction of m-ZrO_2 was estimated as ~ 0.2 using the method reported by the Toraya et al. [27]. As shown in Fig. 1a, introduction of copper into the ZrO_2 lattice resulted in the disappearance of the diffraction peaks of t-ZrO_2 and a shift of the diffraction peaks of m-ZrO_2 to higher 2θ values, pointing to an amorphous or semicrystalline nature of t-ZrO_2 and a substantial incorporation.

In addition, the intensity of the diffraction peaks of CuO intensified with the increase of mol ratio of Cu/Zr, indicating that the dispersion of copper species became worse. The average crystallite sizes of CuO are estimated using Debye–Scherrer equation and are summarized in Table 1. With the increase of the mol ratio of the Cu/Zr, the CuO crystallite sizes of CZ*x* samples increase from 12 to 35 nm, suggesting that some copper species aggregated in the sample with higher copper content.

To investigate the active phase of the Cu/ZrO_2 catalysts, four catalysts were reduced and the XRD patterns of them were shown in Fig. 1b. Only the metallic copper phase can be seen for all the samples, indicating that the bulk CuO in the catalysts was totally reduced to metallic copper. No crystalline phase peak attributed to Cu(I) was observed by XRD. Therefore it is reasonable to believe that the active sites in this reaction must include Cu^0. Supposing the metallic Cu particles are spherical, the average copper metal crystallite sizes can be calculated from the full width at half-maximum (FWHM) of Cu(111) diffraction lines. The results, listed in Table 1, reveal that the average Cu particle size is similar to that of the corresponding CuO for CZ2, while this value is much larger for CZ3 and CZ4. We can afford to believe that the CuO crystalline phase in CZ2

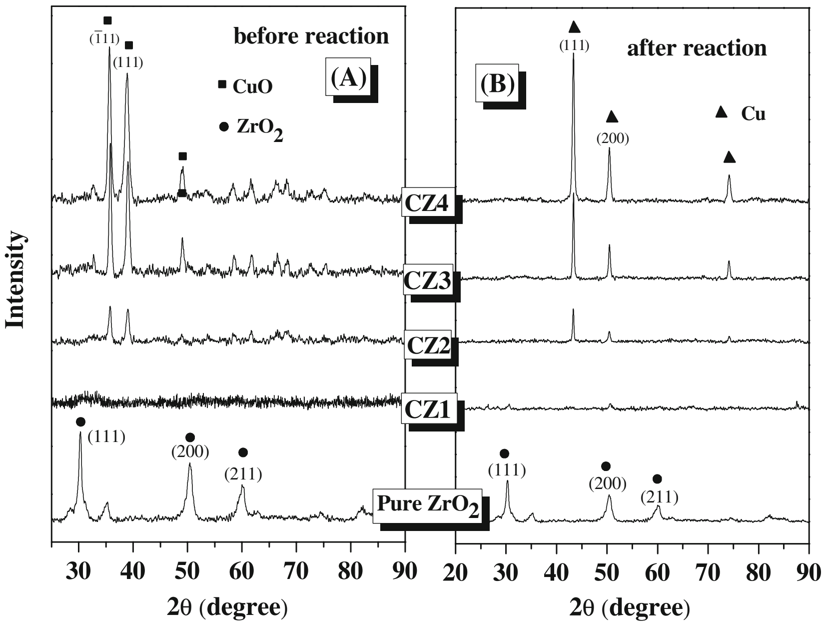

Fig. 1 XRD patterns of CZ*x* catalysts **a** before reaction; **b** after reaction

Table 1 Physico-chemical properties of the CZ catalysts with different Cu/Zr mole ratio

Catalyst	$^{a}S_{BET}$ (m^2 g^{-1})	$S_{Cu}N_2O$ (m^2 g_{Cu}^{-1})^b	$S_{Cu}N_2O$ (m^2 g_{Cat}^{-1})^b	$^{c}d_{Cu}$ (nm)	$^{c}d_{CuO}$ (nm)
CZ1	191.6	34.2	4.1	–	–
CZ2	134.4	44.3	11.5	13.4	12.1
CZ3	88.9	24.5	10.8	24.5	18.7
CZ4	64.5	5.3	3.6	46.3	34.0
ZrO$_2$	215.9	–	–	–	–

[a] BET specific surface area

[b] Active Cu metal surface area determined by N$_2$O titration method

[c] Calculated from the XRD data based on Scherrer equation

precursor is very stable upon reduction and no aggregation took place.

The physico-chemical properties of the calcined the reduced catalysts are also listed in Table 1. With the increase of copper content, the BET surface area of the Cu/ZrO$_2$ catalysts decreased from 191.6 to 64.5 m^2 g^{-1}. However, it is interesting to note that the metallic Cu surface area measured by N$_2$O titration demonstrate clearly that the CZ2 catalyst exhibits the highest copper dispersion when compared with other samples, inferring a unique Cu–ZrO$_2$ metal-support interaction in this sample. It should also be pointed out that CZ2 also shows the highest specific Cu surface area per gram of copper, even much larger than that of CZ1, suggesting its special property, which is in well line with its good catalytic performance.

3.2 TPR

To investigate the reducibility of the copper species in the Cu/ZrO$_2$ catalysts, TPR measurements were performed and the results were illustrated in Fig. 2. In TPR measurements, all samples presented a broad and a narrow peak profile in the range of 453–653 K. The reduction of bulk CuO is featured by a single reduction peak at a considerably higher temperature of 573 K [28, 29] (not shown). It is thus concluded that there is Cu/Zr interaction which facilitates the reduction of the supported copper oxide species. Along with the increase of the zirconium content, the broad peak weakens gradually while the narrow peak swells, indicating that the zirconium composition can remarkably improve the reducibility of the supported copper oxide materials. Many literatures were concerned about the Cu reduction [13], and most of them believed that Cu(II) could be reduced by a two-step transformation. To gain a further insight into the TPR results, a curve-fitting procedure was preformed by a computer program [13]. The peak positions and relative contents derived from the curve-fitting program are summarized in Table 2. The original TPR profile can be deconvoluted to at least two peaks in all samples, suggesting the presence of at least two different states of

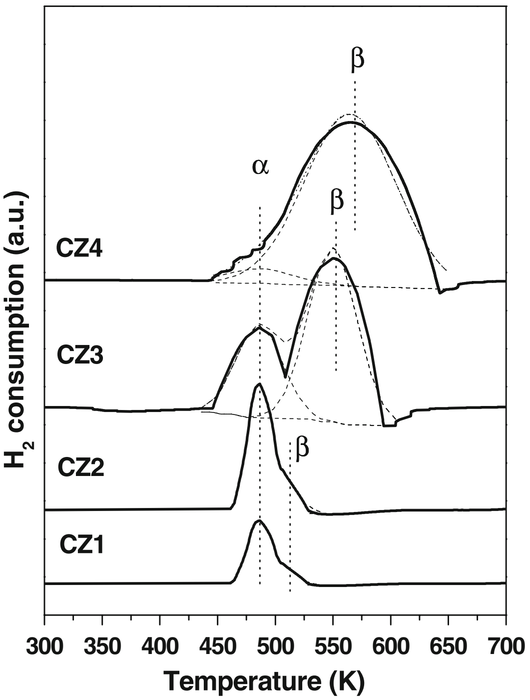

Fig. 2 TPR profiles of CZ*x* catalysts

Table 2 Auger parameters and BEs of the core electrons for CZ*x* catalysts determined by XPS after exposed to various conditions, i.e., (1) calcined catalyst (calc.), (2) reduced in 4 bar 5% H_2/Ar at 523 K for 2 h(red.), (3) after exposure to the O_2/CH_3OH at 523 K(post)

Catalysts	TPR peak position (K) and percent (%)	
	α	β
CZ1	485(68.3)	503(31.7)
CZ2	495(64.8)	502(35.2)
CZ3	486(33.5)	550(66.5)
CZ4	487(5.6)	565(94.4)

CuO in the Cu/ZrO_2 catalysts. It is widely accepted that highly dispersed CuO phase is composed of α peak, and β peak which are ascribed to crystallized copper oxide weakly interacted with the coexisted ZrO_2 surface [30]. The fraction of high temperature reduction peak were observed to be larger and shifted to higher temperatures with the increase of copper content, suggesting different dispersion state of copper species in all cases. Based on this, we can attribute the $\alpha/(\alpha + \beta)$ value to the highly dispersed copper species which has stronger interaction between copper species and the support. In addition, it is interesting to find that the highest area ratio of $\alpha/(\alpha + \beta)$ for CZ2 was observed when compared with CZ3 and CZ4 samples, indicating the presence of the highest content of CuO with strong Cu/Zr interaction in CZ2 sample. Although the intrinsic nature is not clear yet, this character may be one of the factors that influence its catalytic performance. A similar shift of the reduction maxima toward higher temperature has been previously observed by Fierro et al. in a TPR study on the interaction of Cu–Zr system and by Robinson and Mol in a study of the interaction of CuO and ZnO [31], which was both attributed to the presence of a specific type of CuO strongly interacted with the ZrO_2 or ZnO lattice.

It should be noted that CZ2 catalyst displays the lowest reduction temperature of all the catalysts, suggesting the presence of small CuO or Cu particles and thus much higher component dispersion. The TPR results correlate well with the active metallic copper surface area and the XRD measurements (see the context, CZ2 presents the highest dispersion and least CuO and Cu particle sizes). In addition, the main reduction profile of CZ2 is narrow and almost symmetrical, implying that the particle size distribution is narrow.

3.3 XPS

XPS investigation of BEs and intensities of the surface elements provide information on the chemical states and relative quantities of the outermost surface compounds. XPS spectra were collected for CZ*x* catalysts after exposure to various atmospheres, viz. (1) fresh after calcinations in air, (2) after reduction in 1 atm 5% H_2/Ar at 523 K for 2 h, and (3) after exposure to the feed gas of O_2/CH_3OH at 523 K in order to evaluate Cu(II), Cu(I) and Cu^0 proportions on the surface and then to confirm the state of the active species on the Cu/ZrO_2 catalysts. Detailed quantitative results from the peak-fitting results of Cu 2*p* and Cu LMM are also presented in Figs. 3 and 4. The fresh sample calcined at 723 K displayed the main Cu 2*p*3/2 peak at 933.6 eV accompanied with a satellite peak (2*p* → 3*d*) at 943.0 eV. In the pre-catalysts, there is only Cu(II) species present on the surface [23, 24]. Exposed to 5% H_2/Ar and O_2/CH_3OH mixture at 523 K, the satellite peak of the sample disappeared as depicted in Fig. 3, indicating the reduction of the surface Cu(II) to lower oxidation states, i.e., Cu(I) or Cu^0. The distinction between these species is only feasible through the analysis of the modified Auger parameter (defined as $\alpha_A' = h\nu + KE_{LMM} - KE_{Cu\ 2p3/2}$) [32]. In Fig. 4, it is found that every Cu LMM spectrum contains more than one component, which indicates that Cu^0 and Cu^{1+} are coexisting in the catalyst after reduction. After calculation from Fig. 4, Cu^0 molar ratio reaches a maximum (84.8%) after exposure to the O_2/CH_3OH mixture at Cu/Zr mole ratio of 2:3.

All the XPS parameters of the samples investigated and the surface atomic ratios of Cu/Zr in CZ*x* are listed in Table 3. As shown, after exposure to H_2/Ar and O_2/CH_3OH mixture, the surface composition is strongly

Fig. 3 Cu 2*p* X-ray photoelectron spectra of the reduced (**a**) and the post-reaction (**b**) Cu/ZrO_2 catalysts

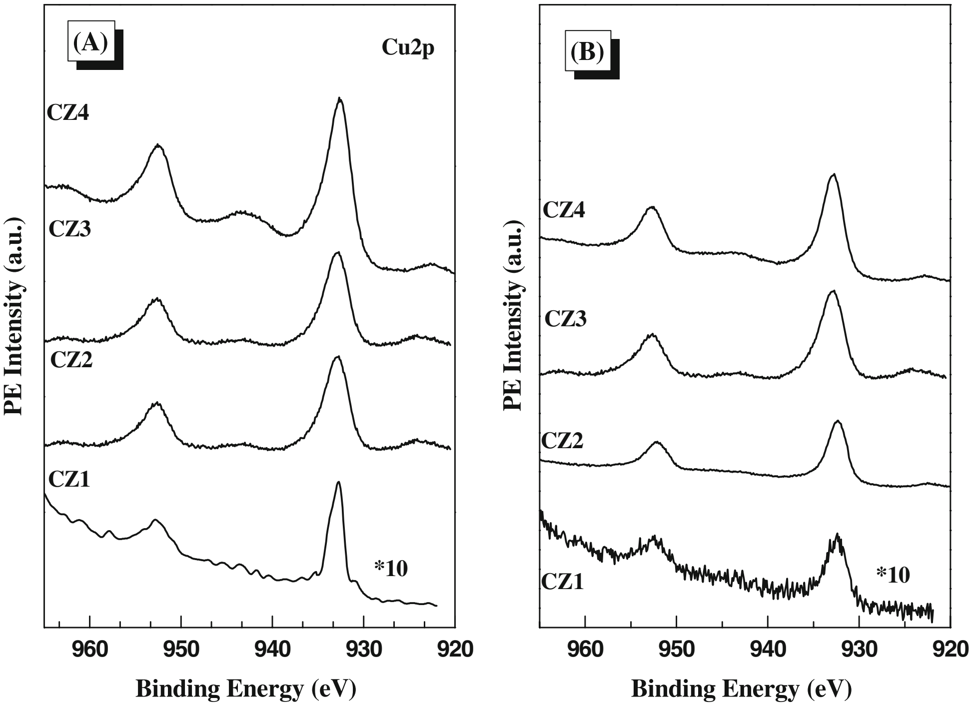

Fig. 4 Cu LMM XAES spectra of the reduced (**a**) and post-reaction (**b**) Cu/ZrO_2 catalysts

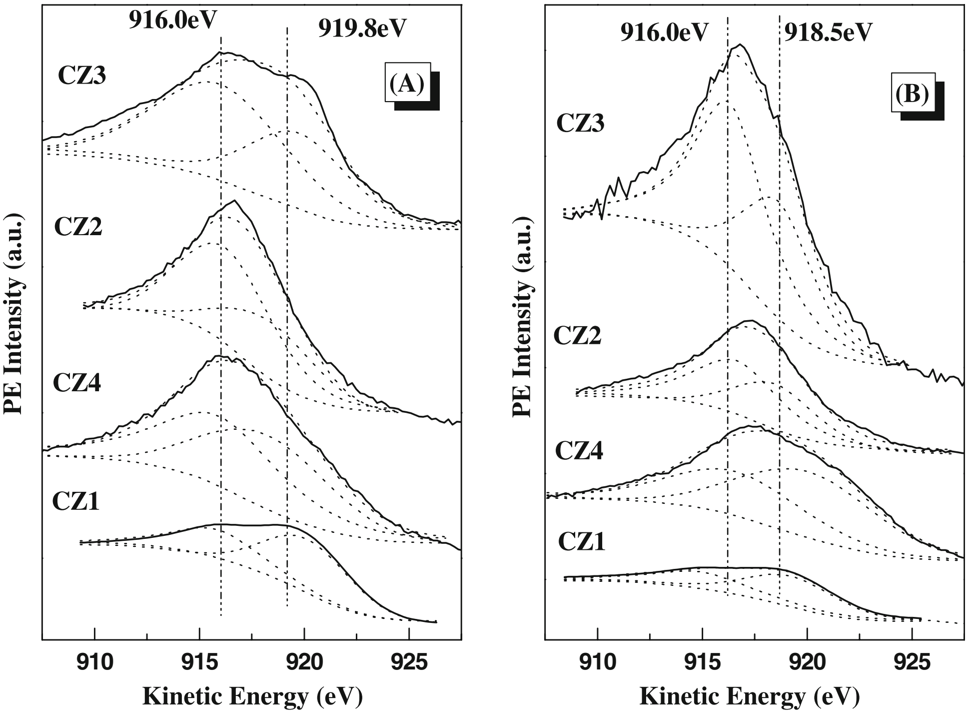

affected by the treated conditions. The surface copper content of CZ2 decreases while the surface copper content of CZ1, CZ3 and CZ4 increases after reduction and then decreases after exposure to the O_2/CH_3OH mixture. When the mole ratio of Cu/Zr is at 2:3, the surface copper content is higher than that of the bulk. However, this value is far lower than that of the bulk in CZ1, CZ3 and CZ4 catalysts, suggesting that CZ2 may show the highest Cu surface area among the four CZ*x* catalysts. It also can be seen that copper is enriched on the surface of CZ2 with a surface

Table 3 Activity and selectivity for POM over CZ*x* catalysts

Sample	State	Cu $2p_{3/2}$ B.E. (eV)	CuLMM K.E. (eV)		Zr $3d_{5/2}$ B.E. (eV)	Cu/Zr mole ratio
CZ1	Calc.	933.8	–	–	182.1	0.12
	Red.	932.8	915.6	918.3	181.8	0.13
	Post	932.9	915.0	918.7	182.8	0.28
CZ2	Calc.	933.4	–	–	182.1	0.88
	Red.	932.9	916.0	918.3	182.3	0.71
	Post	932.9	916.1	918.5	182.3	0.57
CZ3	Calc.	933.5	–	–	181.8	0.64
	Red.	932.8	916.1	919.3	182.9	0.94
	Post	932.5	916.3	918.5	182.1	0.57
CZ4	Calc.	933.7	–	–	182.9	0.80
	Red.	932.8	916.0	918.9	182.2	1.43
	Post	932.4	916.1	918.9	181.9	1.08

Reaction conditions: $O_2/CH_3OH = 0.5$, WHSV $= 3.8\ h^{-1}$, $p = 1$ atm

[a] Hydrogen molecules produced per surface Cu atom per second at 453 K

atomic Cu/Zr ratio of 0.709, as compared with the bulk one at 0.68. However, this ratio decreases after the reduction, suggesting the increase of the crystal size of copper or the encapsulation of copper by zirconium oxide. Similar results were also observed in Cu/Zn, Cu/Al and Cu/Cr systems.

It is known that highly dispersed or bulk CuO with the particle size around 10 nm could be easily reduced to Cu^0 at a relatively higher temperature of 623 K and it is very interesting to find that high surface Cu(I) ratios (all higher than 40%) are observed in the present CZ*x* catalysts, suggesting the super stability of surface Cu(I) in the Cu–Zr system. However, no significant variations were observed in the BEs of Zr 3*d*5/2 in both the sample before and after reaction, indicating that the chemical environment of Zr is stable. According to the results from XRD and XPS for the Cu/ZrO_2 catalysts before and after activity tests, it can be concluded that lower valence Cu were the active species on the surface for POM reaction.

XPS results also show that the surface composition of the present CZ catalysts deviated significantly from the bulk composition. The Cu/Zr mole ratio of the calcined and the used CZ2 sample remained more or less in the same range and shows a correlation with the observed activity and stability. Compared to other CZ catalysts, an optimal Cu/Zr ratio of 2/3 is required to obtain high activity and stability.

3.4 Activity Test

Measurements of catalytic activity for POM were carried out at O_2/CH_3OH mole ratio of 0.5 in the feed. It is found that all the oxygen was consumed when methanol conversion was higher than 20%. In the present POM reaction, hydrogen and carbon dioxide were the main products, and carbon monoxide and water was the main by-products. No other products, such as formaldehyde, dimethyl ether, methyl formate or formic acid, could be detected under the experimental conditions.

Figure 5 gives a typical set of results for POM over CZ2 catalyst and traditional Cu/ZrO_2 catalyst prepared by the sodium carbonate co-precipitation method, illustrating the effects of reaction temperature on the methanol conversion and the selectivity to hydrogen. It is obvious that the methanol conversion increases with the increase of the reaction temperature and can be up to >99% at 533 K and hydrogen selectivity kept around 90% when the reaction temperature was increased from 433 to 533 K. However, compared with the CZ2 catalyst, the traditional Cu/ZrO_2 catalyst exhibits relative worse results, when reaching the same methanol conversion the reaction temperature of the CZ2 catalyst is 40 K lower than the sodium carbonate co-precipitation derived Cu/ZrO_2 on average and the hydrogen selectivity could be up to 88% even at 573 K. It is interesting to find that there is no carbon monoxide detected at 433 K. However, at higher temperature, a trace of carbon monoxide is observed. When the reaction temperature increased from 423 to 533 K, the carbon monoxide selectivity increased from 0 to 1.8% while the selectivity to H_2O decreased ($*\Sigma_H$ also increased), suggesting that MD played some role at high temperature. It is also found that 100% methanol conversion and 91% hydrogen selectivity and less than 1.6% CO selectivity can be achieved over the Cu/ZrO_2 system at a relatively low temperature of 533 K, which is the first good result in this field. The good performance of this novel Cu/ZrO_2 catalytic system implies its further promising industrial application.

To investigate the long-term behavior of the Cu/ZrO_2 catalysts for POM reaction under optimal reaction

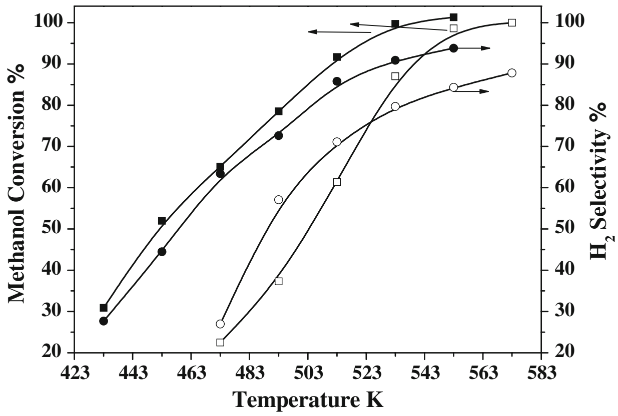

Fig. 5 Effect of reaction temperature on the methanol conversion and hydrogen selectivity over CZ2 catalyst (■, ●) and traditional Cu/ZrO$_2$ catalyst (□, ○) prepared by co-precipitation of Na$_2$CO$_3$. Reaction conditions: O$_2$/CH$_3$OH = 0.5, WHSV = 3.8 h^{-1}, p = 1 atm

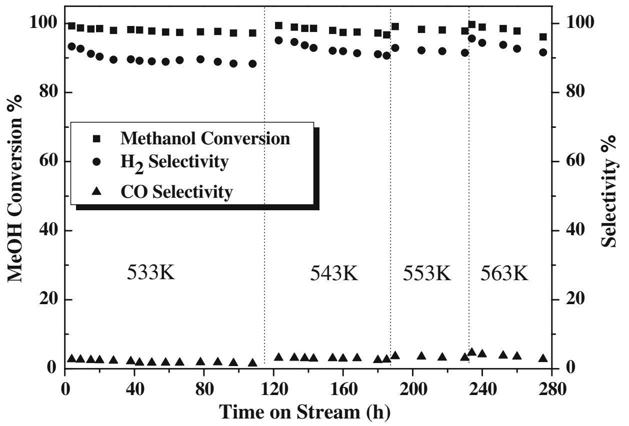

Fig. 6 The durability test of CZ2 catalysts in the POM reaction. Reaction conditions: O$_2$/CH$_3$OH = 0.5, WHSV = 3.8 h^{-1}, p = 1 atm

conditions, a life-time test was carried out on the CZ2 catalyst and Fig. 6 shows the deactivation trend during 533–563 K. It is found that the novel Cu/ZrO$_2$ catalyst exhibits good stability. Only little deactivation in a 280 h test was observed while previous Cu/Zn/Cr catalyst deactivated obviously during a 100 h test [7]. Life time experiments reported by Alejo et al. [10] show that Cu$_{40}$Zn$_{55}$Al$_5$ is stable during the partial oxidation of methanol with no significant change in activity and selectivity even after 110 h operation at 503 K while the catalyst Cu$_{40}$Zn$_{60}$ with no alumina deactivates rapidly after 20 h reaction at 503 K, and further life time experiment more than 110 h is not provided. Cu–Cr catalyst may have good stability in the partial oxidation of methanol; however, the toxicity of Cr is not fitted for the requirements of green chemistry. Cu/ZrO$_2$ catalyst reported by Yao et al. [3] showed good catalytic performance in the steam reforming of methanol, but its application in the partial oxidation is the first time. Two main problems using Cu/ZnO/Al$_2$O$_3$ catalyst are the stability of the catalyst activity in time on stream against the temperature and CO formation in product stream, which can deteriorate the Pt electrode and the fuel cell performance, even at a very low concentration. During our research processing, the precipitator is found to have a great influence on the catalytic performance of the partial oxidation of methanol. The sodium hydroxide–sodium oxalate-assisted Cu/ZrO$_2$ catalyst exhibits good catalytic performance and catalyst stability; even after 280 h life time experiment the catalyst still can maintain high methanol conversion and hydrogen selectivity. Such result is higher than those reported in the literatures.

It is also very interesting to find that the CO selectivity did not increase over the present CZ2 catalyst, suggesting its potential as a good candidate in industry. Much smaller extent of deactivation was identified in the Cu/ZrO$_2$ catalyst, which could be attributed to the fact that the copper was stabilized by zirconia and copper particles in the bulk zirconia are less inclined to agglomerate during the POM reaction.

Table 4 summarizes the methanol conversion, selectivity to hydrogen and CO, hydrogen production rates, and turnover frequencies (TOFs) for the POM reaction over the different CZx catalysts. Note that the activity data shown in Table 4 were obtained at 493, 513 and 533 K. For POM, the temperature increase will be helpful to make the equilibrium transfer to the hydrogen and CO$_2$, and, however, much higher temperature will lead to the decomposition of the methanol and the oxidation of hydrogen to water. To obtain higher hydrogen selectivity, proper temperature was desirable. Among the CZx catalysts, the CZ2 catalyst shows the highest methanol conversion, the highest hydrogen selectivity and the lowest CO selectivity. In particular, the CZ2 catalyst exhibited the best performance in terms of hydrogen generation velocity. It is remarkable that the methanol conversion of 91.7% could be obtained over the CZ2 catalyst at 493 K, much higher than those over CZ1 (58.3%), CZ3 (85.3%) and CZ4 (54.5%). Moreover, the startup temperatures of Cu/Zr catalysts are also much different. The CZ2 can show considerable methanol conversion and hydrogen selectivity at 443 K while the other CZx catalysts nearly initiated around this temperature, suggesting the excellent low temperature startup property, which is very useful for PEMFC. In addition, at 453 K, CZ2 shows the highest TOF value among the four catalysts, indicating that the active site in the present Cu/ZrO$_2$ system is a structural-sensitive one. A certain Cu/Zr ratio (2:3) can lead to the most active copper site.

Table 4

Catalyst	T (K)	MeOH conv. (%)	H_2 selec. (%)	CO (%)	H_2 gen. velocity ($cm^3\ g^{-1}\ min^{-1}$)	TOF[a] ($10^3\ s^{-1}$)
CZ1	493	58.3	49.0	0.4	55.3	51
	513	68.3	72.5	0.5	95.8	
	533	87.1	79.7	1.1	134.4	
CZ2	493	78.5	72.4	0.9	110.0	126
	513	91.7	85.8	1.1	152.3	
	533	99.7	90.9	1.8	175.4	
CZ3	493	70.9	75.1	0.5	103.1	84
	513	85.3	81.7	1.1	134.9	
	533	94.8	88.2	1.4	161.8	
CZ4	493	54.5	49.3	2.1	52.0	40
	513	75.2	74.2	2.5	108.0	
	533	89.1	79.2	3.3	136.6	

3.5 Discussion

Zirconium supported copper catalyst was considered as an interesting catalytic material. It has been generally accepted that catalysts containing copper and ZrO_2 behave in a bi-functional manner in methanol synthesis reaction. An investigation of in situ FTIR by Fisher and Bell revealed the involvement of similar bi-functional roles of copper and ZrO_2 in the MD method [18]. Accordingly, methanol interacts with the OH groups of ZrO_2 to form water and methoxide, leading to dehydrogenation into formaldehyde and subsequent decomposition to gaseous CO_2 and H_2 generation. The main role of copper is to accept the surface species located on ZrO_2 and subsequent desorption of molecular hydrogen [17]. Besides, ZrO_2 is known to possess anionic vacancies, which entails a geometric effect that can influence the dispersion and lead to a change in the morphology of the supported metallic copper particles [22]. Considering the present Cu/ZrO_2 catalyst prepared by the sodium oxalate assisted coprecipitation method, large amounts of anionic vacancies or defects formed during the calcination process with the decomposition of the sodium oxalate in this study, which may enhance the adsorption of the methanol, therefore, the catalytic performance was enhanced in the POM reaction. Rhodes and Bell [33] reported that Cu/*m*-ZrO_2 is nearly an order of magnitude more active for methanol synthesis than Cu/*t*-ZrO_2 for equivalent zirconia surface area and surface concentrations of dispersed Cu, for a given phase of zirconia, the methanol synthesis activity increases linearly with the surface concentration of Cu. In our present preparation method, after introduction of copper species, the diffraction peaks of *t*-ZrO_2 disappeared and only remained those of *m*-ZrO_2, indicating that the introduction of copper species inhibited the formation of crystalline *t*-ZrO_2 or made them amorphous or semi-crystalline. Considering these unique features rendered by the ZrO_2 in the supported catalytic systems, it is reasonable that the binary CZ*x* catalyst system, in particular the one prepared by sodium hydroxide–sodium oxalate-assisted co-precipitation, shows excellent catalytic performance.

It is known that methanol conversion over copper based catalysts during the POM greatly depends on the status of copper, such as the dispersion, metal surface area and particle size. Generally, catalyst with higher copper dispersion shows better catalytic performance in the POM reaction, whereas the status of metal dispersion is closely related to overall surface area. Unfortunately, the Cu/Zr-based catalysts reported in the literature generally have a limited copper surface area by conventional preparation methods. In the present work, we have demonstrated that the sodium hydroxide–sodium oxalate-assisted co-precipitation method can allow the generation of a new type of Cu/ZrO_2 catalysts with a much higher specific surface area and improved copper dispersion with respect to its conventional counterparts. As a result, the CZ catalyst obtained by sodium hydroxide–sodium oxalate-assisted co-precipitation method exhibited a unique catalytic behavior in POM reaction as compared to the catalysts prepared by other methods (not shown here) in terms of methanol conversion, H_2 generation and CO concentration.

Considering the essential nature of metallic copper for the catalytic generation of hydrogen from POM, some studies have experimentally demonstrated that for a given type of catalyst, the catalytic activity is directly proportional to the metallic copper surface area [6]. However, there are also conflicting reports which suggest that the methanol conversion or hydrogen generation rate cannot be correlated to the surface area of metallic copper for the Cu-based catalysts [15]. It is therefore very interesting to make a comparison between the catalytic activity of the present CZ*x* catalysts of different Cu/Zr mol ratios and the metallic copper surface area obtained from N_2O titration. Figure 7 shows the effect of different Cu/Zr mol ratios on the

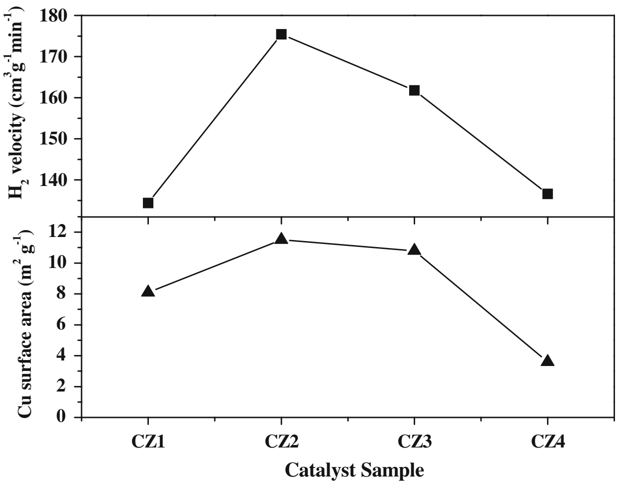

Fig. 7 Hydrogen-production rate ($cm^3\ g^{-1}\ min^{-1}$), specific active copper surface area as a function of mole ratio of Cu/Zr

hydrogen generation velocity as well as the specific surface area as determined by surface titration with N_2O. As shown in Fig. 7, the variation in copper specific area shows an excellent correlation with the corresponding hydrogen generation velocity, indicating that the active Cu surface area contributes mainly to the catalytic activity of Cu/ZrO_2 in the POM reaction. Special attention must be paid to consider that the catalytic activity may also be related with the phase of ZrO_2. Although the effect of the m-ZrO_2 on the catalytic behavior is still not clear, the role it plays can not be neglected. Relevant research will be studied in the future.

From the present investigation, it can be seen that the good catalytic performance of the sodium hydroxide–sodium oxalate-assisted Cu/ZrO_2 catalyst may be attributed to the higher copper surface area. Furthermore, the improved synergy effect between active Cu material and ZrO_2 as a consequence of a higher component is also thought to be essential for the enhanced catalytic performance in the POM reaction. It should also be noted that the most active catalyst CZ2 shows the largest TPR peak of $\alpha/(\alpha + \beta)$ as compared to other CZx catalysts, which indicates that the stronger interaction between copper species and support also helps to improve the catalytic performance of the POM reaction. Previous investigations concerning the reducibility of copper based catalysts for methanol synthesis have revealed that a better reducibility is always associated with a higher activity of the catalyst.

4 Conclusions

The present study demonstrates novel Cu/ZrO_2 catalysts prepared by sodium hydroxide–sodium oxalate-assisted co-precipitation, which is highly active and stable in the POM. The mole ratio of Cu/Zr has great influence on the catalytic behavior in the POM. The good catalytic performance and long-term stability of the Cu/ZrO_2 catalysts could be attributed to the high copper species dispersion on zirconium components and high active specific copper surface area with a much stronger Cu–Zr interaction as well as a beneficial synergy of m-ZrO_2 promotion as confirmed by results from TEM, XRD, N_2O titration, H_2-TPR and XPS.

Acknowledgments This work was financially supported by the Major State Basic Resource Development Program (Grant No. 2003CB615807), NSFC (Project 20573024), and the Science & Technology Commission of Shanghai Municipality (08DZ2270500, 06JC14004).

References

1. Agrell J, Birgersson H, Boutonnet M (2002) J Power Sources 106:249
2. Ahmed S, Krumpelt M (2001) Int J Hydrogen Energ 26:291
3. Yao CZ, Wang LC, Liu YM, Wu GS, Cao Y, Dai WL, He HY, Fan KN (2006) Appl Catal A 297:151
4. Vankova S, Tsoncheva T, Mehandjiev D (2004) Catal Commun 5:95
5. Tsoncheva T, Vankova S, Mehandjiev D (2003) Fuel 82:755
6. Matter PH, Braden DJ, Ozkan US (2004) J Catal 223:340
7. Wang Z, Xi J, Wang W, Lu G (2003) J Mol Catal A 191:123
8. Wang Z, Wang W, Lu G (2003) Int J Hydrogen Energ 28:151
9. Cubeiro ML, Fierro JLG (1998) Appl Catal A 168:307
10. Alejo L, Lago R, Pena MA, Fierro JLG (1997) Appl Catal A 162:281
11. Agrell J, Germani G, Jaras SG, Boutonnet M (2003) Appl Catal A 242:233
12. Agrell J, Boutonnet M, Fierro JLG (2003) Appl Catal A 253:213
13. Velu S, Suzuki K, Okazaki M, Kapoor MP, Osaki T, Ohashi F (2000) J Catal 194:373
14. Turco M, Bagnasco G, Costantino U, Marmottini F, Montanari T, Ramis G, Busca G (2004) J Catal 228:56
15. Turco M, Bagnasco G, Costantino U, Marmottini F, Montanari T, Ramis G, Busca G (2004) J Catal 228:43
16. Eswaramoorthi I, Sundaramurthy V, Dalai AK (2006) Appl Catal A 313:22
17. Fisher IA, Bell AT (1999) J Catal 184:357
18. Fisher IA, Bell AT (1998) J Catal 178:153
19. Fisher IA, Bell AT (1997) J Catal 172:222
20. de Lima SM, Cruz IO, Jacobs G, Davis BH, Mattos LV, Noronha FB (2008) J Catal 257:356
21. Eduardo W (2007) US Patent 2007269367
22. Pokrovski KA, Bell AT (2006) J Catal 244:43
23. Robert S, Thorsten R, Frank G, Herry P, Reinhard S, Markus A, Hendrik SJ, Rachel C, WO2004083116
24. Oguchi H, Kanai H, Utani K, Matsumura Y, Imamura S (2005) Appl Catal A 293:64
25. Ritzkopf I, Vukojevic S, Weidenthaler C, Grunwaldt J, Schuth F (2006) Appl Catal A 302:215
26. Chen HW, Yin AY, Dai WL, Fan KN (2009) Acta Chim Sinica 2:129
27. Toraya H, Yashmura M, Somiya S (1984) J Am Ceram Soc 67:119
28. Liu Z, Amiridis MD, Chen Y (2005) J Phys Chem B 109:1251
29. Caballero A, Morales JJ, Cordon AM, Holgado JP, Espinos JP, Gonzalez-Elipe AR (2005) J Catal 235:295

30. Fierro G, Lo Jacono M, Inversi M, Porta P, Cioci F, Lavecchia R (1996) Appl Catal A 137:327
31. Robinson WRAM, Mol JC (1991) Appl Catal A 76:117
32. Campos-Martin JM, Fierro JLG, Guerrero-Ruiz A, Herman RG, Klier K (1996) J Catal 163:418
33. Rhodes MD, Bell AT (2005) J Catal 233:198